Triplet exciton migration in a conjugated polyfluorene

Carsten Rothe* and Andy P. Monkman
OEM Research Group, Department of Physics, University of Durham, Durham, DH1 3LE, England
(Received 4 April 2003; published 25 August 2003)

The diffusion and triplet energy relaxation in amino endcapped poly [9,9-bis(2-ethylhexy1)fluorene-2,7-diyl] has been studied using photoluminescence and photoinduced absorption, both time-resolved covering ten decades of time, dependent on temperature, excitation dose, and concentration. The results are analyzed employing the concept of dispersive hopping in a Gaussian distribution of states (DOS), characterized by width δ of 40 meV. It is found that the initial photogenerated triplet population in the polymer films decays fairly equally by triplet-triplet annihilation and intrinsic monomolecular decay, respectively. In the latter case, the triplet excitons survive the initial 100 ms either in trap states outside the DOS at ambient temperature or within the DOS at low temperature. Further, it is clearly found that triplet migration in this conjugated polymer is both an intrachain and interchain process. Interchain hopping of triplet excitons must occur, which subsequently leads to the observation of delayed fluorescence. The nature of interchain hopping of the triplets is discussed.

DOI: 10.1103/PhysRevB.68.075208 PACS number(s): 78.66.Qn, 78.55.−m, 33.50.Dq

I. INTRODUCTION

Conjugated polymers have attracted considerable research interest during the past decade due to their great potential in applications such as electrically pumped lasers and solar cells, but mainly as active materials for displays. The latter, being based on polymer light-emitting diodes (PLED), are thought to combine economical production with superior properties when compared to the current technologies. Generally two types of excited species are formed in working PLED's potentially emissive singlet states and nonemissive triplet states. Theoretically the branching ratio favors the triplet state 3:1 due to the statistical nature of the recombination process of the carriers. However, spin-dependent recombination suggests a ratio closer to 1:1, depending on the individual polymer.[1] The implications of this clearly show that triplet states have equal importance compared to the singlet state. However, there is much more known about the fluorescent singlet exciton. This fact is understandable bearing in mind that the triplet is, due to spin conservation, highly nonemissive, which impedes its observation with almost every direct luminescence measurement. For experimental studies the triplet manifold is usually populated via photoexcitation followed by intersystem crossing (ISC), which is more or less efficient depending on the conjugated polymer.[2] In principle, short current pulses could alternatively serve as an excitation source, which was recently shown by Sinha *et al.*[3] However, the latter method has some disadvantages regarding triplet migration studies. First of all, the current source is, in practice, a voltage source, thus the initial charge-carrier density, concomitantly the triplet density, is unknown. Further, the comparatively long excitation pulses limit time resolution, charge carriers remain, which might influence the triplet concentration long after excitation, and the technique is restricted to thin films. Thus, for the present study pulsed laser excitation is deemed the superior method.

Nevertheless, monitoring the phosphorescence (Ph), originating from the radiative (spin-forbidden) decay of the first excited triplet to the singlet ground state, $T1 \rightarrow S0$, is, independent of the excitation mechanism, possible in the long-time region after excitation, e.g., >10 ms, when combined with low temperature. This very low time resolution is not due to a lack in sensitivity but follows from the long radiative lifetime of the triplet state in pristine conjugated polymers. As an example, from the radiative lifetime of the triplet, roughly 1 s, it follows that only every 100 000th triplet created would decay radiatively in the first 10 μs. Aggravating this, the ISC rate (for photoexcitation) and the phosphorescence quantum efficiency are far from unity, hence temporally resolved phosphorescence detection at early times after excitation is impossible. Even at intermediate measurement times, (μs to ms) the Ph signal is superimposed on the strong delayed fluorescence (DF), whose low-energy tail extends into the spectral region of the Ph emission. Thus a study of triplet migration in conjugated polymers cannot only rely on the photoexcited phosphorescence observation because the migration of the triplet excitons is much faster compared to their radiative lifetime. In those conjugated polymers in which the DF after photoexcitation originates from triplet-triplet annihilation (TTA) of course the latter contains information about the precursor triplet states as well and therefore studying the DF offers a powerful tool for gaining information about the triplet state, especially in the first 10 ms after excitation.

Employing gated spectroscopy techniques at low temperature, Romanovskii *et al.* observed both Ph and DF, emitted by the conjugated polymer methyl-poly(paraphenylene) (MeLPPP).[4] Recently, similar observations have been reported for polyfluorenes[5–7] and polythiophenes.[8] For the present photoluminescence study a polyfluorene derivate was chosen, since here the DF originates undoubtedly from TTA,[9,10] whereas the analysis of photoemission experiments under applied bias voltage suggests the DF of MeLPPP to be caused by delayed charge-carrier recombination.[11] The emphasis of this investigation is to examine the known experimental observations in greater detail and thus gain deeper insight into the nature of the triplet state in conjugated polymers in general. Special attention is focused on the migration and annihilation of triplets and on their lifetimes at various

temperatures including the important case of thin films at room temperature. To do this, mainly the DF kinetics of the polymer were investigated as a function of temperature and excitation dose in different environments covering solution, frozen solution, film, and blended into an inert matrix polymer. The results obtained were further complemented by time-resolved transient triplet absorption studies and analyzed in the framework of a well-established migration theory relying on the hopping of localized particles in a distribution of energy states.

II. EXPERIMENT

The synthesis of the polyfluorene derivative poly [9,9-bis (2-ethylhexyl)fluorene-2,7-diyl] endcapped with *N*,*N*-bis(4-methylphenyl)-*N*-phenylamine (PE2/6am4) (see inset of Fig. 2 below for chemical structure) is described in the literature.[12] We chose this polymer rather than a more common polyfluorene because it shows much less tendency to form ketodefect sites. In order to investigate the concentration dependence of the decay kinetics, dilute solutions of PF2/6am4 in either 2-methyltetrahydrofuran (MTHF), methylcyclohexane (MCH), or toluene have been prepared. The polymer fractions were 10^{-3}, 10^{-4}, and 10^{-5} by weight, which for the lowest concentration corresponds to a $\approx 5 \times 10^{-6}$-mol repeat unit/mol solvent. After transferring the solutions into a sealed degassing cell, attached to a quartz cuvette, the air dissolved in the solutions was removed by three freezing-pumping cycles. Additionally, MTHF and MCH/toluene form clear glassy matrices at low temperature making possible the investigation of low polymer concentrations imbedded in a rigid matrix. To do so, a sealed cylindrical quartz viewport, loaded in our glove box under a nitrogen atmosphere, containing predeoxygenated polymer solution, was attached to the cold finger of a temperature-controlled displex helium cryostat (lowest temperature $\approx$15 K).

A disadvantage of frozen solution is its natural restriction to low temperature. This limitation has been circumvented by imbedding the investigated polymer into zeonex—a cyclo-olefine, from ZEON. In order to fabricate films, zeonex containing 10^{-4}- or 10^{-5}-by-weight PE2/6am4 was dissolved in toluene and subsequently drop cast onto silicon wafers. With this procedure we obtained perfectly clear films exhibiting the purple color of PF2/6am4 solutions. To compensate for the low absolute absorption of these (thin, dilute) films, typically 20 films where stacked together forming one sample of about 2-mm overall thickness.

Additionally, solid polymer films have been prepared by spin coating a 0.02% by weight solution of PF2/6am4 in toluene onto previously cleaned quartz substrates. For the present time-resolved spectroscopy studies a pulsed Nd: yttrium aluminum garnet laser (pulse width 120 ps; maximum pulse energy at the excitation wavelength 355 nm, 7 mJ; repetition rate 1–10 Hz) was used to excite the singlet manifold of PF2/6am4. The light emitted by the sample was monochromated and subsequently detected by our gated intensified charge coupled device (CCD) camera (4 picos, Stanford Computer Optics). ''Gated'' refers to an adjustable time delay after the trigger pulse (provided by a fast photodiode responding to the excitation laser) set before the start of detection, with the duration of detection also being tunable (the time resolution is limited by a minimum gate width of 200 ps). However, this highly sensitive CCD camera provides a useful dynamical range of only three orders of magnitude. Hence, measuring a signal drop of some 15(!) orders of magnitude lasting up to ten decades in time is still a challenge. In this context measurements with a fixed gate are not feasible, hence, gate widths were applied, which increased dynamically with the time delay. In practice, a set of delay times (t_x) was chosen to cover the desired time region equally spaced on a logarithmical scale. The gate time was a tenth of the delay time, hence the measured intensity at point t_x can be expressed as

$$I_{t_x}^{\mathrm{meas}} \propto \int_{-t_x/20}^{+t_x/20} I(t)\,dt, \tag{1}$$

with $I(t)$ being the true time-dependent intensity. In order to normalize the gate widths the data points were scaled by t_x^{-1}. It should be mentioned that the measurement is a differential experiment, since for every gate/delay time pair the former is much shorter than the latter. The above procedure immediately yields the true kinetics and integration is not necessary. Finally, in order to smooth laser intensity fluctuations, every spectrum (measure point) was obtained by accumulating up to 50 laser shots. Sometimes whole decay curves were taken several times in order to circumvent long-time laser intensity fluctuations.

Complementary to emission studies the triplet decay kinetics have additionally been probed using time-resolved transient photoinduced triplet absorption (TRA). An advantage of this method is that the signal, defined as a normalized change in the probe transmission T, is directly proportional to the triplet density n, $-\Delta T/T = n\,\delta d$, where d is the sample thickness and δ the excitation cross section. In order to excite the polymer the same pulsed laser used for the emission detection served as the pump beam in the transient absorption experiment. The probe beam was provided by an intense infrared light-emitting diode (760 nm), whose emission matched the wavelength of the transient triplet absorption of PF2/6am4. Having passed either the liquid or solid sample attached to the cold finger of our displex helium cryostat, the probe beam was detected by a fast silicon pin diode. Using a current amplifier (200-MHz bandwidth) the signal was then converted into voltage and monitored by a 300-MHz digital oscilloscope. For the whole setup an excellent signal-to-noise ratio ($\Delta T/T = 10^{-4}$) was achieved, accompanied by a poor time resolution of 1 μs. In order to cover the initial time regime, another complementary TRA experiment was carried out employing the gated CCD camera. Here the probe beam was provided by a stabilized tungsten lamp to record TRA spectra. Unlike the above experiment the signal-to-noise ratio was poor ($\Delta T/T = 10^{-2}$); however, this was compensated by the time resolution, which is, in principle, identical to the CCD shortest gate width, 200 ps. In practice, spectra earlier than 50 ns could not be obtained as a consequence of the strong fluorescence of the investigated polymer, which has a spectral contribution even at 1.6 eV superimposed on the

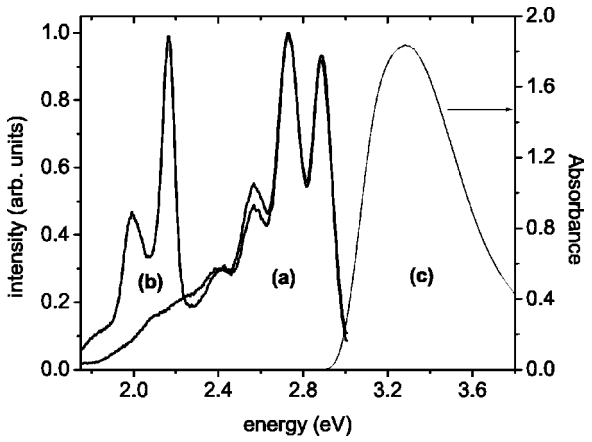

FIG. 1. Normalized prompt and delayed emission spectra of a PF2/6am4 film at 15 K. The delayed fluorescence appears identical in spectral position and shape to the prompt fluorescence (a). Additionally, but only detectable for long gate times, phosphorescence is emitted peaking at 2.17 eV (b). For comparison the 300-K absorption spectrum of the same film is included (c).

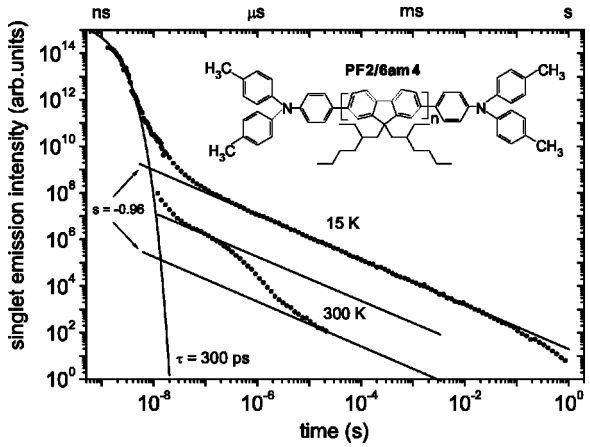

FIG. 2. Double logarithmic time-dependent singlet emission of 10^{-4} polymers imbedded into zeonex. For the sake of clarity the 300 K is offset by two orders of magnitude compared to the 15-K curve. The solid lines correspond to algebraic decays with a slope -0.96 and to exponential kinetics with 300-ps decay time, respectively. The chemical structure of the end-capped polyfluorene, PF2/6am4 derivative, used throughout this study, is depicted in the inset.

TRA signal. This is a fundamental property of this special polymer and does not appear for weakly emissive materials.

III. RESULTS

In Fig. 1 the isoenergetic prompt (PF) and delayed fluorescence (DF) as well as the redshifted phosphorescence (Ph) spectra are shown as observed at 15 K. For the purpose of comparison the 300-K absorption spectrum of a spin coated film is also shown. The curves are consistent with data published for similar polyfluorene derivates,[5,9] in particular, confirming that the different end groups do not alter the photophysics. Even if the spectral appearances of the (normalized) PF and DF are identical, the intensity difference between both kinds of emission is remarkable—some ten orders of magnitude for the spectra presented in Fig. 1. Representing the numerous decay curves measured for this study, two typical temporal decay patterns of the (spectrally) integrated DF obtained from zeonex films are presented in Fig. 2 in a double logarithmic fashion. The spectra of Fig. 1 represent roughly the start point and end point of the upper curve of Fig. 2. Apparently the kinetics are far from being simply monoexponential and, depending on experimental parameters such as temperature, up to seven time regimes exhibiting different decay kinetics are distinguished as follows.

Extending over the initial 4 ns, the tail of the PF is visible, featuring a monoexponential decay, which was simulated using a 300-ps characteristic lifetime, see the upper curve of Fig. 2. This (slightly temperature-dependent) PF lifetime of PF2/6am4 agrees well with data previously obtained.[13]

Extending over the next 100 ns after photoexcitation a fast decaying DF (subsequently called DF1) is visible, which obeys a power-law decay with a slope between -2 and -3. This emission, which to our knowledge has not been mentioned in the literature before, is truly delayed rather than the tail of the PF, as the double logarithmic graph might suggest. For example, at 20 ns the measured intensity is $\sim 10^{10}$ times stronger than that expected from the exponential PF decay (compare with exponential simulation). There are many reasons not to assign the origin of this kind of DF to TTA. One is the laser excitation dose dependency shown in Fig. 3, which was measured for a 10^{-4} MCH solution. Here, gate windows were chosen such that the intensity dependencies are obtained selectively for the PF, DF1, and the subsequent long-time DF. The clearly linear dependence for the early, fast DF1 component on excitation power points to a monomolecular rather then bimolecular origin, such as TTA. The latter findings are identically recovered in films and solutions. However, since the present study is devoted to the

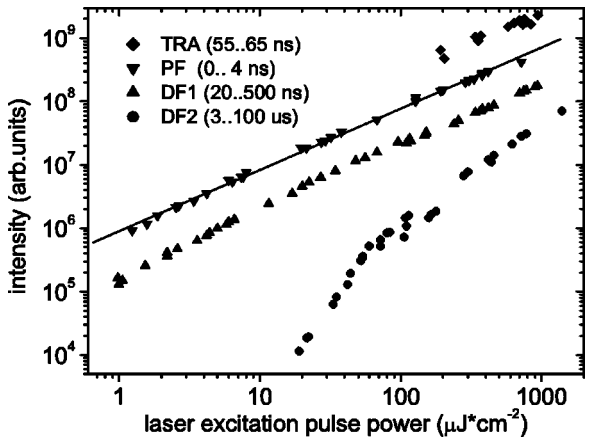

FIG. 3. Laser power dependency of (from top to bottom) transient triplet absorption (TRA), prompt fluorescence (PF), early time (DF1), and late time delayed fluorescence (DF2) components. The measurements have been taken using a 10^{-4} MCH solution at 300 K rather than a film. In order to see that the gate times employed indeed correspond to DF1 and DF2, refer to the solution decay kinetics shown in Fig. 6. The solid line depicts a linear increase with laser power.

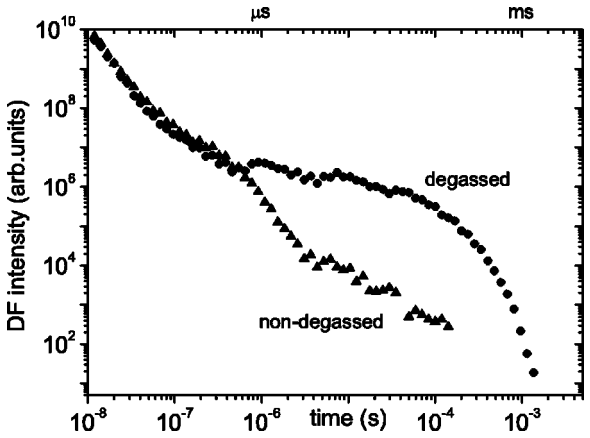

FIG. 4. The effect of oxygen on the DF decay kinetics of a 10^{-3} toluene solution at 300 K. The curves are non-normalized, thus, at variance to DF1 only DF2 is affected by oxygen. The curves start to separate after a delay of 600 ns.

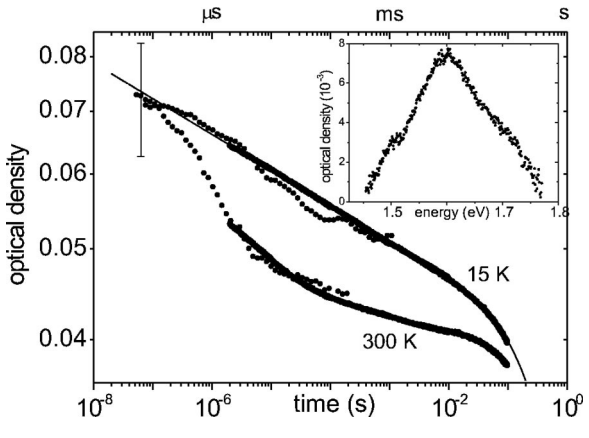

FIG. 5. Time-resolved transient triplet absorption signal of 10^{-4} polymers in zeonex at 15 and 300 K. The curves are composed of two data sets obtained independently with a CCD camera and oscilloscope in order to cover the initial and late time regimes, respectively. The CCD camera results are smoothed; an error bar of the original data is given. The solid line fit of the 15-K curve corresponds to Eq. (2). The inset shows a TRA spectrum at 15 K, which was obtained using the CCD camera.

triplet state we do not deal with this kind of DF here, and a detailed characterization will be given in a forthcoming publication.

With delay times exceeding the DF1 regime, the DF (hereafter called DF2) decay becomes slower, obeying an algebraic law with slope -0.96 ± 0.01 in the case of zeonex and thin films. A slightly faster decay is found for all kinds of frozen solutions -1.13 ± 0.01 (upper part of Fig. 7 below). We emphasize that these slopes within the given error limits have been observed without exception (20 times for films and zeonex; 4 times for different frozen solutions), therefore they represent firm results rather than random derivations from an ideal slope of -1 caused by inaccuracies of measurement. For sufficiently high temperatures, e.g., the 300-K curve in Fig. 2, we see a turning point $[t_{s(300\,\mathrm{K})}\approx 200\,\mathrm{ns}]$ after which the decay becomes faster, again exhibiting slopes of ~ -2. These general decay patterns were always observed in zeonex as well as for polymer films and the frozen solution. This kind of delayed emission (DF2) originates from TTA, which was shown independently by Hertel *et al.* and ourselves.[9,10] For example, the bimolecular nature of the annihilation process manifests itself in superlinear excitation dose dependencies as shown in the lower curve of Fig. 3. Naturally any additional triplet decay besides TTA will result in reduced DF2 emission intensities. This is the reason for the accelerated DF2 decay for delay times >100 ms, e.g., seen in the upper curve of Fig. 2, since here the radiative triplet decay (Ph) becomes increasingly important.

Turning our attention to the DF decay in Fig. 4, we find that liquid solution is the only exception in which the typical algebraic behavior of DF2 kinetics is not observed at all. In this case, DF2 decays monoexponentially, featuring typical lifetimes of 1 ms. However, we do observe the algebraic law upon freezing these solutions. The transition from the exponential curve of Fig. 4 towards the more complicated decay shown in the upper curve of Fig. 7 below occurs smoothly at intermediate temperature. It is worth mentioning that this changeover is accompanied by a roughly thousandfold increase of the initial DF2 emission intensity. Thus the rather weak DF2 intensity observed at room temperature becomes comparable to the emission intensity of thin films upon freezing the solution. The DF2 intensity of liquid solutions is heavily reduced in the presence of a triplet-quenching oxygen concentration, as demonstrated by Fig. 4. Note that the decay curves presented are not normalized, thus there is no oxygen effect on the fast DF1, further confirming that triplets are not the origin of DF1.

The inset of Fig. 5 shows a transient triplet absorption (TRA) spectrum of a 10^{-4}-wt% polymer in zeonex. The peak energy position for PF2/6am4 is blueshifted by $\sim$150 meV compared to photoinduced absorption spectra of a similar polyfluorene derivate poly(9.9-dioctylfluorene),[14] but has a similar spectral appearance. The main part of Fig. 5 compares the temporal decay of the TRA signal at 15 and 300 K, measured using a zeonex film. As described in Sec. II the data points are combined from two different experiments: whereas the noisy initial points represent integrated TRA spectra obtained with the CCD camera, the later time region is covered by an oscilloscope trace. At first glance the triplet decay patterns resemble those of the DF2, see Fig. 2. However, in the same time regime in which the DF2 intensity decreases by some eight orders of magnitude the TRA signal is only reduced by approximately 30%. This is not an inconspicuous inconsistency. If TTA is the only depletion mechanism for the initially created triplet reservoir, then the resulting DF2 kinetics are proportional to the change of the number of triplets in time rather than being directly proportional. The low-temperature, time-dependent TRA signal (upper curve of Fig. 5) can be fitted extremely well using a simulation of the form

$$Ph(t)\propto t^{-s}\times e^{-t/\tau}. \tag{2}$$

The characteristic radiative triplet decay lifetime τ is found to be 1.43 s. This value slightly exceeds the phosphorescence decay time, 1.1 s, found by Hertel *et al.* for a similar polyfluorene derivate in frozen solution.[9] However, the authors

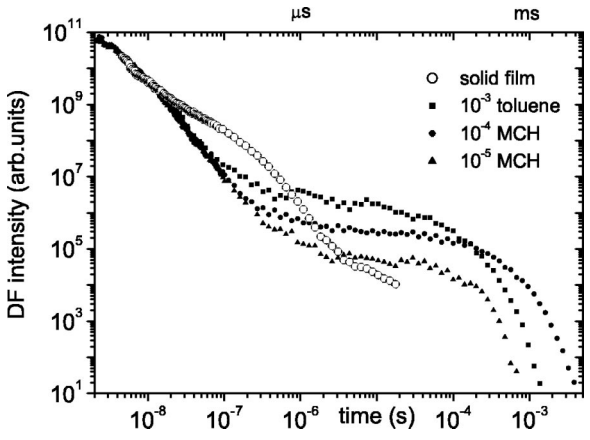

FIG. 6. DF2 decay kinetics at 300 K of three solutions containing different polymer concentrations (lower curves). The laser pulse power was fixed to 100 μJ/cm^2. The emissions are scaled to the DF1 signal, thereby accounting for the reduced absorption at lower polymer concentrations. For comparison a typical solid film decay at 300 K is plotted as well.

assumed only exponential triplet decay thereby neglecting the additional algebraic component, hence a smaller exponential decay time is expected. In Eq. (2) the exponent s describes the power-law contribution to the triplet decay. Due to the high number of data points provided by the averaged digital oscilloscope trace (>2000) this exponent is found with low error limits, $s=-0.039\pm0.001$. Unlike the DF2 kinetics, the latter value does not depend on whether frozen solution, zeonex, or polymer films have been investigated; recall that the algebraic DF2 slopes are -0.96 and -1.13 for zeonex or thin film and frozen solution, respectively. At variance to the DF kinetics, the weak time dependence (slope -0.04) of the triplet decay also extends into the first 100 ns, thereby confirming the lack of any sort of fast initial decay comparable to the DF1 kinetics. This observation once more proves that, unlike the DF2, the DF1 does not originate from TTA. However, the turning point in the DF2 kinetics from slope ~-1 to -2 is accompanied by a similar change in the TRA curve at the same (temperature-dependent) delay time t_s. This observation might be visualized by comparing the 300-K zeonex curves of Fig. 2 (DF) and 5 (TRA); in both cases $t_s\approx200$ ns. After t_s the TRA signal declines by some 25% (relative to the slope of -0.04). Then the decay again slows down until the radiative triplet lifetime becomes dominant. Likewise, this long-lasting tail has its counterpart in the DF2 kinetics. It is worth mentioning that none of the TRA features described above could be observed in liquid solution. Here the TRA, proportional to the triplet concentration, decays monoexponentially (not shown) as does the DF2 signal in the same environment. In particular we did not observe any long-lasting (>10 ms) tail, thereby confirming the lack of any trapped, nonemitting triplet population in liquid solution.

In Fig. 6 the room-temperature DF decay is shown for a solid polymer film and a (liquid) solution at three different polymer concentrations c. These curves are scaled to the DF1, which is directly proportional to the PF (see Fig. 3), and the initial created singlet concentration, respectively. We

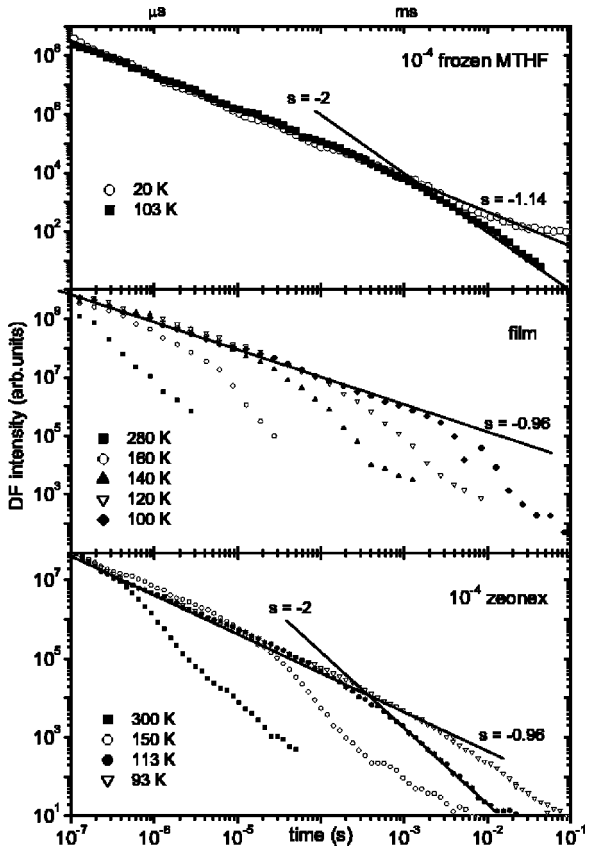

FIG. 7. Compendium of non-normalized decay curves at different temperatures for a 10^{-4} frozen solution, film, and 10^{-4}-by-weight PF2/6am4 in zeonex. Note that at long delay times a relatively strong Ph compared to the DF2 disturbs the 20-K frozen solution curve.

find that with increasing concentration more DF2 is emitted relative to the (de facto normalized) absorption. Expressed in absolute numbers the DF2 intensity relative to the laser absorption is reduced by a factor of 6 for a tenfold dilution of the polymer, DF2$\sim c^{1.8}$.

A compendium of decay curves obtained from frozen solution, thin film, and zeonex film at several temperatures is shown in Fig. 7 on a common time axis. First of all, we note that these curves are not normalized. Therefore the DF2 intensity is almost temperature independent as long as the -0.96 slope regime is valid. Obviously the accelerated decay of the DF2 starts earlier with increasing temperature, and, concomitantly, the turning point shifts to shorter delay times after photoexcitation.

Finally, we remark that it is impossible to obtain equally meaningful kinetics in the same temperature range for a liquid or frozen solution, due to the transition from exponential towards algebraic DF2 decays upon cooling the solution described above. Having characterized the major DF regimes we now turn our attention to a side observation. Looking at the DF2 and here on the time region just before the turning point (e.g., for the 150-K zeonex curve of Fig. 7 around 1 μs) the delayed emission intensity is enhanced relative to the -0.96 slope. Due to the double logarithmic presentation this intensity increase looks inconspicuously small, however, it

actually amounts to a ~50% increase in intensity. This behavior is very visible if the DF2 intensity is plotted versus temperature for a fixed delay time, as was shown previously.[10]

IV. DISCUSSION

The elementary step of exciton migration in conjugated polymers is the incoherent jump between localized energy states, which constitute a material-dependent density distribution of states (DOS). Initially created at random within the DOS, the excitons relax towards the tail states in the course of their random walk. This thermalization renders the diffusion time dependent, making the mathematical treatment more complex than in the case of organic crystals. Thus, for our data analysis we draw heavily on the results of earlier mathematical work[15–17] about nonequilibrium diffusion and energy relaxation in localized state distributions, which were confirmed by Monte Carlo simulations.[18–20] In the framework of these theories, motion is governed by the Miller-Abraham equations describing the jump rate between two localized states separated by R_{ij},

$$\nu_{ij} = \nu_0 e^{-2\alpha R_{ij}} e^{-\varepsilon_j - \varepsilon_i / k_B T}, \quad \varepsilon_j > \varepsilon_i,$$

$$\nu_{ij} = \nu_0 e^{-2\alpha R_{ij}}, \quad \varepsilon_j < \varepsilon_i, \tag{3}$$

where ν_0 is the attempt-to-jump frequency, which is close to a typical phonon frequency $\sim 10^{12}$ s^{-1}, and α denotes the inverse localization length. If these theories are applied to organic systems, a Gaussian distribution is always the best choice to describe the DOS,

$$n(\varepsilon) \sim e^{(\varepsilon - \varepsilon_T)^2 / 2\delta^2}, \tag{4}$$

with δ being the variance (width) of the distribution and ε_T the center energy.

Let us briefly outline the scenario of bimolecular triplet annihilation after pulsed photoexcitation followed by intersystem crossing. In general an excited triplet density (n_0) is depopulated by monomolecular decay processes (k; impurity quenching and radiative decay) combined with bimolecular annihilation (γ):[21]

$$\frac{dT}{dt} = n_0 - kT - \gamma T^2. \tag{5}$$

If we assume that nonradiative quenching is not a major decay mechanism and further consider only the early time period after (pulsed) photoexcitation (for PF2/6am4, $t < 100$ ms) we can neglect the monomolecular term, thus considering bimolecular annihilation to be the only decay mechanism. It follows that the DF observed at a delay time t is directly proportional to the triplet decay at the same time:

$$\mathrm{DF} \sim \frac{dT}{dt} = -\gamma T^2, \tag{6}$$

therefore the triplet density decays according to

$$T(t) = \frac{n_0}{1 + \gamma n_0 t}$$

or in general, for time-dependent γ,

$$T(t) = \frac{n_0}{1 + n_0 \int_0^t \gamma(u)\, du}. \tag{7}$$

According to Smoluchowski's theory of bimolecular reactions (in the asymptotic time-independent limit) the annihilation constant γ is proportional to the triplet diffusion coefficient (D), the interaction radius (R), and the fraction of triplets annihilated after encounter (f),[22]

$$\gamma = 8\pi f R D. \tag{8}$$

Equations (6)–(8) have been applied successfully for several organic crystals, which exhibit an isoenergetic site distribution. Typical values reported for γ and D are 10^{12} cm^3 s^{-1} and 10^4 cm^2 s^{-1}, respectively.[23] However, one of the main results of the treatment of migration in an energetic distribution of states was that the diffusion coefficient D itself is time dependent rather than a constant. The diffusion evolves in two time regions from nonequilibrium towards an equilibrium diffusion regime. The former is characterized by thermalization of the triplets, initially created at random energy, towards tail states of the DOS, which is accompanied by a rapid decrease of D. In the subsequent equilibrium regime, the triplet migration is governed by thermally assisted jumps and the diffusivity adopts a constant value D_∞. Indeed, throughout this study (film, zeonex film, and frozen solution) the triplet population (monitored by the TRA experiment) in the nonequilibrium time regime decays as $t^{-0.04}$ rather than t^{-1}, as expected from Eq. (7) for time-independent diffusion. Plugging this measured triplet slope into Eq. (7) for time-dependent diffusion yields the time dependence of the annihilation constant and, hence, of the triplet diffusivity as γ, $D \sim t^{-1.04}$. If we check for self-consistency and substitute the latter dependence into Eq. (6) we obtain an expected time dependence for the delayed fluorescence caused by TTA, $DF \sim t^{-1.12}$. This is in truly excellent agreement with the DF2 slopes observed in frozen solution, $t^{-1.13 \pm 0.01}$. However, there is a slight but unambiguous discrepancy when compared to the film or zeonex film slopes, which is discussed in detail later. First, we examine with priority whether the diffusion time dependence agrees with the theoretical framework. From this point of view, the exact behavior of $D(t)$ is strongly dependent on the DOS relative to the available activation energy, e.g., the temperature of the environment, and is not trivial to cast into an explicit analytical expression for a Gaussian energy distribution. Nevertheless, in an attempt to solve the migration problem analytically in the zero-temperature limit Movaghar, Ries, and Grunewald derived an expression for the time dependence of the average hopping rate,[16] which is directly proportional to the diffusivity and thereby to the triplet-triplet-annihilation constant γ:

$$\gamma(t) \sim D(t) \sim \nu(t) \sim \frac{1}{t \ln(\nu_0 t)}, \tag{9}$$

which can be approximated by $\nu(t) \sim t^{-1.04}$ in the long-time limit.[20] Thus our experimentally derived $\gamma(t)$ is not a random material-dependent function but is in fact exactly the expected diffusion time dependence for any Gaussian DOS in the $T \rightarrow 0$ limit. It is worth mentioning that in this case the diffusivity never reaches its equilibrium value, e.g., migration is carried out by downhill jumps in energy only. The latter fact can be rationalized bearing in mind the absence of any thermal phonons. However, for finite temperature the long-time diffusivity does settle to its equilibrium value D_∞. In other words, the system reaches its quasiequilibrium after a temperature-dependent delay time t_s, which was shown analytically using an effective-medium approximation,[24] and confirmed employing Monte Carlo techniques, for example, by Ref. 18:

$$t_s(T) = t_0 e^{(c\delta/k_B T)^2}, \tag{10}$$

where c is a constant depending on the dimensionality of the migration; $c = 0.93$ or $\frac{2}{3}$ for one- or three-dimensional migration, respectively.[25] t_0 is not just the inverse attempt to jump frequency ν_0 from Eq. (3) but denotes the dwell time for triplets in PF2/6am4 migrating through a hypothetical isoenergetic ($\delta = 0$) equivalent structure. Thus, both parameters are related to each other by

$$t_0 = [6\,\nu_0 e^{(-2\alpha R_{ij})}]^{-1}. \tag{11}$$

For the study of transient particles, a certain temperature region (for the PF2/6am4 triplet $\lesssim 90$ K) exists in which equilibrium diffusion might be reached from the point of migration; however, this is impeded by the finite monomolecular lifetime of the particles. Once quasiequilibrium has been established, the retarding effect of D on the triplet annihilation rate γ vanishes. Therefore, the delayed fluorescence and the surviving triplet population decay, with their ''classical'' slopes -2 and -1, respectively, according to Eqs. (6) and (7). For example, the acceleration of the DF decay is clearly observed in Fig. 7, where it obeys a power law with slope -2 after a temperature-dependent turning point. Regarding the TRA signal, the situation is complicated by a residual signal, whose origin is discussed in detail later.

Now we draw attention to the compendium of turning times t_s versus inverse squared temperature, plotted in Fig. 8 in a semilogarithmic fashion according to Eq. (10). The values were obtained from the intersections of -0.96 and -2 slopes fitted to the appropriate time regimes in the DF2 kinetics. Within experimental error a linear behavior is found. A least-squares fit yields $\delta = (41 \pm 1)$ meV (for three-dimensional migration) and an intersection with the $1/T^2$ axis at $t_0 = (70 \pm 20)$ ns. Recently, Hertel *et al.* investigated the temperature dependence of the DF turning points of a polyfluorene derivative imbedded into frozen MTHF, between 100 and 130 K.[9] These authors analyzed their data according to Eq. (10) but obtained a slope with rather different parameters, which is included for comparison as a dashed line in Fig. 8. However, since the glass transition temperature of MTHF is below 100 K, the solvent does not act as a true rigid matrix in this temperature regime, thus TTA is artificially accelerated. This explains the unphysically low value for t_0 obtained. For the same reasons Fig. 8 does not contain any frozen solution data points for temperature higher than 100 K.

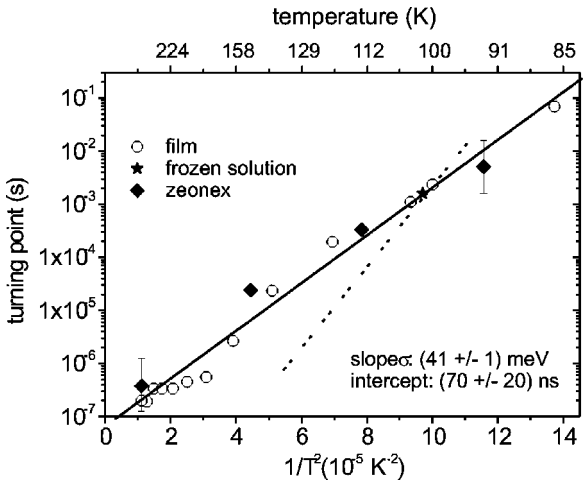

FIG. 8. The turning point of several DF2 decay curves (among others taken from Fig. 7) as a function of the inverse squared temperature according to Eq. (10). The true turning point is assumed to lie within one order of magnitude in time around the values found in Fig. 7, indicated by the error bars. The dashed line corresponds to data obtained experimentally by Hertel *et al.* (Ref. 9).

An independent measure of δ can also be gained employing a Gaussian profile analysis of the high-energy tail of the inhomogenously broadened $T1 \rightarrow S0$ phosphorescence spectrum. To do so it would be necessary to examine the unrelaxed Ph spectrum at zero time delay because in the course of relaxation the Gaussian distribution narrows. Unfortunately, it is experimentally not possible to observe an instantaneous Ph spectrum as a consequence of the long radiative triplet lifetime, therefore δ cannot be measured directly. Nevertheless, in Fig. 9 the baseline-corrected Ph spectrum from Fig. 1 was analyzed yielding FWHM $= 61$ meV and $\delta^t = 25.9$ meV, respectively. This Ph spectrum was taken at 15 K, corresponding to a disorder parameter of $\hat{\delta} = (\delta/k_B T)$

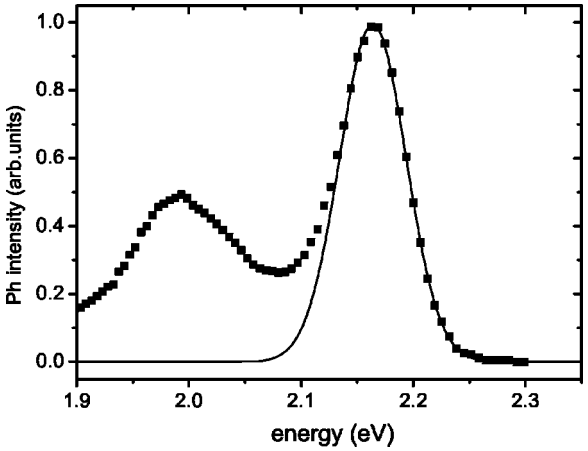

FIG. 9. Baseline-corrected 10-ms delayed Ph spectrum from Fig. 1. Its first vibronic mode is fitted to a Gaussian curve with a FWHM $= 61$ meV (solid line).

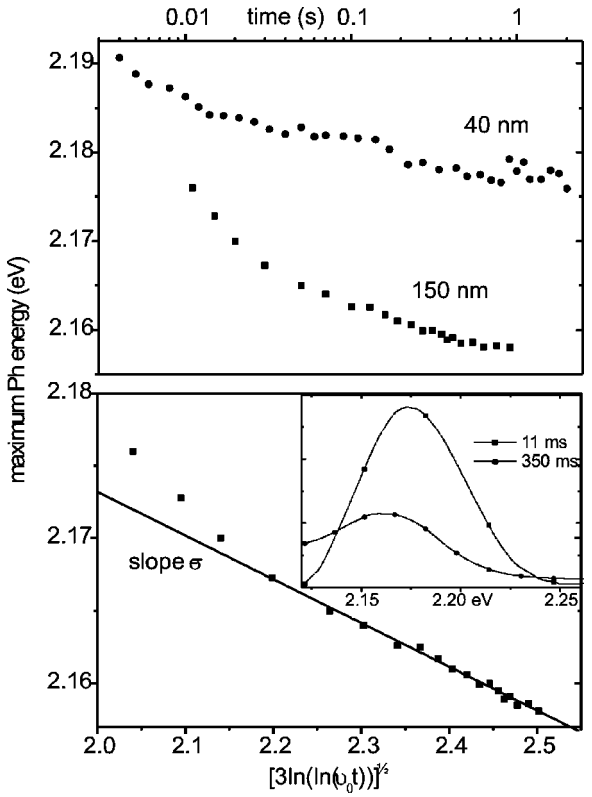

FIG. 10. Upper half: Ph shift versus logarithmic time for two different films. Lower half: thick-film dataset plotted again versus double logarithmic time according to Eq. (12). Data points were derived from Gaussian fits to the first vibronic of 15-K Ph spectra taken with increasing delay. The inset shows two typical Ph spectra after different delay.

>20. Under such conditions, known as the strong disorder case, the Gaussian distribution narrows by $\sim 70\%$ of its initial value as $t \rightarrow \infty$.[26] Thus our experimentally observed distribution (after the elapse of five decades of normalized time) $\delta^t \sim 0.65\delta$ is an expected and reasonable result.

In the theory of migration within an energetic site distribution another aim, besides the time dependence of the diffusivity, was to describe energy relaxation towards the tail states of the DOS with time and temperature. In the last paragraph, the dwell time and the Gaussian width for triplet migration in PF2/6am4 could be gained from the temperature-dependent analysis of the diffusivity (derived from the annihilation rate). Hence, in the following we verify whether the parameters obtained also account for experimentally accessible energy shifts. In the upper half of Fig. 10 the maximum energy of several phosphorescence spectra taken at 15 K with successively increasing delay times, obtained by fitting to a Gaussian shape, is plotted versus time for two polymer films, which possess different thicknesses. The graph proves that triplet relaxation is sensitive to the film thickness, which clearly confirms the interchain nature of triplet migration. This important fact is further validated by the absolute extent of the energy shift compared to δ, since much less energy relaxation is expected in the case of one-dimensional migration.[27,28] At 15 K the case of strong disorder, defined by $\hat{\delta} > 10$ (in our case fulfilled for $T < 48$ K), applies, therefore we again employ the analytical $T \rightarrow 0$ treatment of Movaghar, Ries, and Grunewald, predicting a temperature-independent relaxation of the average energy relative to the center of the Gaussian DOS, which in a simplified version, yields[16]

$$\varepsilon(t) \sim -\delta[\ln(\ln \nu_0 t)]^{1/2} \quad \text{as} \quad t \rightarrow \infty. \tag{12}$$

This asymptotic dependence was confirmed by Ries and Bassler using Monte Carlo techniques.[20] In the lower half of Fig. 10, the center energies of the $T1 \rightarrow S0$ transition of the thicker film have been replotted according to Eq. (12). Consistent with the theory,[16,20] the energy relaxation is faster in the initial time regime (in fact, most of the relaxation is expected to happen between 7 and 700 ns, e.g., $0.1-10t_0$) and turns into an asymptotic linear behavior for long times described by Eq. (12). The exact version of Eq. (12) (please refer to Refs. 16 and 19) also contains a site concentration dependence, which explains the thickness dependence of the energy relaxation of the polymer films studied. In connection to Eq. (12) it has been shown that different site concentrations can be accounted for by a linear scaling of the attempt-to-jump frequency ν_0 to an effective time-scaling factor that includes the site concentration.[19] According to this approach we varied ν_0 until the slope of Fig. 10 yielded $-\delta$. The interception of this linear fit with the energy axis yields the nonrelaxed triplet energy $\varepsilon_T = (2.26 \pm 0.01)$ eV, which is of course slightly higher than the $T1 \rightarrow S0$ band shown in Fig. 9. Consistently, the same value is obtained for the thin-film data set but of course using another ν_0. This triplet energy is in excellent agreement with the value found for polyfluorene in pulsed radiolysis experiments, 2.3 ± 0.1 eV,[29] bearing in mind that the latter result was obtained using a solution at room temperature, thus bathochromic shifts can be expected.

In contrast to the strong disorder case, in which the diffusivity never approaches an equilibrium value, for intermediate disorder the average triplet energy settles δ^2/k_BT below the center of the DOS after equilibrium has been reached, e.g., for $t > t_s$.[30] Therefore plotting the $T1 \rightarrow S0$ maxima versus inverse temperature should, in principle, provide an easy and independent possibility for determining δ. Unfortunately, in our case the onset of equilibrium is accompanied by efficient TTA, causing rapid triplet decay. Consequently, in analogy to the initial Ph spectra but for different reasons, the observation of relaxed Ph spectra is prevented as well. In Fig. 11, the center energies $\varepsilon(T)$ obtained from the experimentally accessible Ph spectra are plotted versus temperature together with the declining Ph intensity (fixed delay, 10 ms). In the equilibrium time domain $\varepsilon(T)$ should decrease proportional to $1/T$. This criterion is obviously not met since $\varepsilon(T)$ decreases monotonically upon raising the temperature, which confirms the nonequilibrium nature in the whole temperature region covered for times up to at least 10 ms, the delay time used to take the Ph spectra. From Fig. 8 one would expect to approach equilibrium at ~ 93 K. The mean energy of the relaxed DOS should then be shifted by $-\delta^2/k_BT \sim 210$ meV relative to ε_T. Note that choosing a longer or shorter delay time would still not enable the obser-

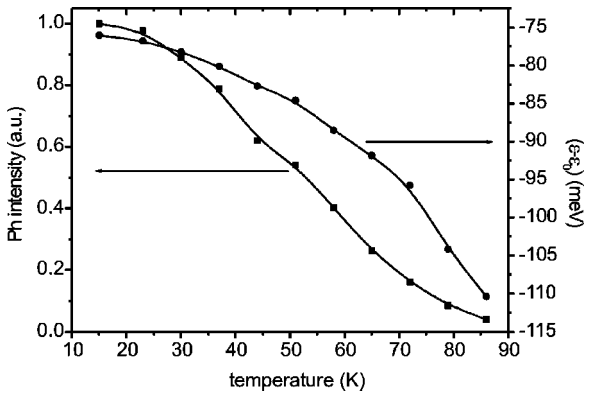

FIG. 11. Ph intensity (squares) and absolute (including the shift that already occurs during the delay time) energy shift (circles) as a function of temperature. Data points were derived from Gaussian fits to the first Ph mode of 10-ms delayed spectra.

vation of the energetically relaxed Ph spectra, but would only shift the onset of equilibrium to lower or higher temperatures, respectively.

Having recognized that on the whole our results are in good agreement with predictions of theories relying on hopping motion in an energetic distribution of states, we now discuss some minor discrepancies. First, recall the DF slopes for frozen solution and films in the strong disorder case, -1.13 and -0.96, respectively. Whereas the first value almost exactly reflects the expected slope of -1.12, the latter gradient exhibits small, but clear deviations given our low error levels. Triplet traps outside the DOS might account for these observed discrepancies. The conversion rate from free triplets into trapped ones would have the same time dependence as the annihilation rate[31] because the diffusivity is rate limiting here as well. Therefore both processes balance in time, making it possible to see DF, which still obeys a power law but with a smaller slope. This, however, has no effect on the TRA signal if we assume that both trapped and free triplets have the same absorption oscillator strengths, which explains the unaltered TRA slope of -0.04.

There are indeed further observations supporting a triplet trap concentration outside the DOS. Kadashchuk *et al.*, using thermally stimulated charge-carrier recombination, very recently demonstrated this for PF2/6.[7] It was found that the trap concentration strongly depends on the film preparation conditions. Another indication for trap sites is the DF2 emission, which exhibits a weak and long-lasting tail beyond the t^{-2} decay. Hertel *et al.* suggested delayed charge-carrier recombination in order to explain a similar kind of DF in polyfluorene.[9] However, in the same temperature-dependent time regime a large triplet density is simultaneously present, confirmed by the TRA signal in Fig. 5. Thus it is more likely that the remaining trapped triplets undergo long-distance tunneling jumps inside another, deeper energetic distribution of trap sites, thereby creating the tail DF2. Finally, we note the modulated continuous-wave TRA experiments by Epshtein *et al.*[32] In agreement with our findings they also proposed that a trap density gave rise to long-lived excitons at room temperature. The much higher laser excitation doses employed in this TRA study enable complete trap filling, observed as a saturated long-lived signal. However, we remark that the untrapped, i.e., migrating triplets are never probed in these quasi-cw experiments (at room temperature) since it would require modulation frequencies of $\sim$10 MHz.

So far we can only speculate about the nature of these traps. However, the fact that the DF decay slope of -0.96 was accurately recovered in diluted zeonex as well as in several pure films suggests a common structure as the trap site. Unfortunately, we were unable to gain any conclusive emission spectrum of the trapped triplets, which could provide an indication about their origin. However, the amine end cap can be ruled out, since the same behavior is found in non-end-capped PF2/6 by Hertel *et al.*[9]

The TRA data shown in Fig. 5 reveal the fate of the triplets quantitatively. Almost independent of temperature half of the initial triplet population survives long enough to decay monomolecularly, the other half being annihilated in the initial 100 ms. However, the processes leading to these decay patterns differ completely in both cases: At low temperature, triplet diffusion is continuously decreasing due to the nonequilibrium nature of migration. This retards triplet-triplet annihilation but also prevents the triplets from arriving at trap sites. At high temperature, TTA proceeds faster as soon as the diffusivity has reached its equilibrium value and triplet diffusion is no longer slowed down. However, this comparably fast diffusion entails that triplets are more likely to migrate to trap sites. As mentioned above, unlike low temperatures, the detection of Ph at room temperature, e.g., emission originating from trapped species, turned out to be unsuccessful, suggesting a vanishing radiative quantum yield for these trapped species. Here we shall remark that the observed relative contributions of the TTA and monomolecular triplet decay (one-half each) cannot be considered as a material immanent property since there obviously exists an intensity dependence. In accordance with Eq. (5), more DF2 is emitted relative to the Ph for increasing laser dose intensities, which concomitantly leads to a reduced average (or effective) triplet lifetime.[18,33] However, this does not alter the functional DF2 decay but only causes a parallel shift in the log-log presentation. Please refer to Ref. 18 for a detailed discussion of this issue.

It was shown above that triplet energy relaxation is dependent on film thickness, which confirms that triplets can overcome the interchain barrier. Now we further illuminate the importance of interchain migration, since common opinion only considers intrachain triplet migration in conjugated polymers. Triplet-triplet annihilation is a short-range exchange process, which relies on the wave-function overlap of the two triplets concerned.[21] Therefore, an essential precondition for the occurrence of DF2, which originates from TTA, is the existence of more than one triplet on a polymer chain. In this context, we now discuss the DF2 concentration dependence shown in Fig. 6. During this experiment, the laser dose was held constant to guarantee an unchanging average number of triplets per chain. Apparent from the graphs, which are normalized to the linearly increasing prompt fluorescence, the DF intensity does increase approximately quadratically with chain density. This experimental result shows that triplets do migrate between neighboring chains and sub-

sequently annihilate. Further, this polymer chain dependency clearly indicates the negligible influence of intrachain sequential triplet production for this material, which is often discussed as a triplet generation mechanism to explain femtosecond photoinduced absorption results.[34] In line with these conclusions is the laser dose dependency of Fig. 3, which rises strictly linearly for the prompt fluorescence. In order to rationalize these findings, one should bear in mind the usually much higher (roughly 100 times) photoexcitation intensities applied in femtosecond studies. Also, triplet fission[35] plays no role here since the triplet energy of PF2/6am4 is 2.26 eV and all experiments were made using 355-nm (3.5-eV) excitation energy, thus to provide enough excess energy to a singlet exciton in order for it to split into two triplet excitons one would have to excite above 274 nm (4.52 eV). Having confirmed an interchain component of the DF2, intrachain TTA between triplets initially created on the same chain could still yield a contribution. However, the average molecular weight of the PF2/6am4 investigated, 29 200 g/mol, corresponds to a chain density of $\approx 1.5 \times 10^{14}$ cm^3 for the 10^{-5}-by-weight diluted polymer. The absorption at the laser excitation wavelength, 355 nm, of such solutions is 0.8 (for one centimeter path length). Therefore the maximum laser excitation dose used for this study, 1 mJ/cm^2, as a first approximation homogeneously absorbed throughout the sample, corresponds to approximately ten initially created singlets per chain. Employing the intersystem-crossing rate for polyfluorene in solution, 0.03[2], on average approximately only 0.3 triplets per chain are created. Because the latter estimate is an upper limit for the initial triplet density per chain (calculated for the maximum laser dose; the typical laser dose was ten times less, ~ 80 μJ/cm^2) we can safely rule out that intrachain TTA is the main contribution to the observed DF2. If one considers the PF2/6am4 polymer chain to be a semirigid coil in solution, from light-scattering data[36] one can calculate the collisional transfer rate of polymer chains (carrying the triplets) in solution using the Einstein-Smoluchowski relationship.[33] For two polymer chains at 1.5×10^{14} cm^3 this encounter rate is ~ 2 s^{-1} and therefore too slow to cause the observed 1-ms exponential triplet decay. Thus any transfer must result from entangled chains or at the instant of excitation closely spaced chains in solution. In fact, the very weak DF2 observed in solution confirms that unlike in films, TTA is not a major quenching mechanism for the triplets, which is justified by the slow polymer chain diffusivity—a necessary precondition for TTA. Furthermore, we know from the solution TRA signal that all triplets are truly quenched rather than occupying nonemitting trap sites like they do in films. Consequently, we conclude that the 1-ms exponential triplet decay in solution is caused by the diffusion of a diluted triplet quencher, which together with the solvent, encounters the polymer chain (the triplets) at a rate of 10^3 s^{-1}. Without further comment, we remark that the triplet quencher does not have to be oxygen.

Surprisingly, upon freezing solutions, $\sim 10\,000$ times more DF2 is emitted in the initial time period, accompanied by a change in the decay kinetics from a relatively slow monoexponential decay at room temperature to the typical fast t^{-1} decay at low temperature. The laser dose was unchanged and so was the initial average triplet number per chain. This strong DF2 emission as well as the TRA results confirm that TTA is a major decay mechanism at low temperature, responsible for $\sim 50\%$ of the triplet decays. Therefore we have to conclude that triplets initially created at neighboring polymer chains annihilate each other. This can only mean that, unlike in room-temperature solutions, in frozen solution the polymer chains form clusters or aggregates, thus the case of isolated chains *no longer* holds true. To our knowledge, no temperature-dependent light-scattering experiments have been done but one can assume that the solubility of the polymer in a certain solvent is reduced upon lowering the temperature, which could in the extreme case lead to phase-separation effects.

Exactly the same holds true for the zeonex films, which might be considered as a frozen solution as well. We know for certain that 10^{-2}-by-weight (1%) PF2/6am4 blended into zeonex forms clusters, which is evident from the opaque appearance and the absorption spectra of these films. Initially we hoped to achieve truly isolated polymer chains upon reducing the amount of PF2/6am4 in zeonex to 10^{-4} and 10^{-5} by weight. However, even in these perfectly clear films TTA occurs at a high rate once equilibrium diffusion has been reached, which is confirmed by the strong TRA decrease. Thus we conclude that the PF2/6am4 chains imbedded in zeonex cannot be considered to be truly isolated either.

Subsequently, we are able to discuss another experimental result, which is surprising at first glance but can easily be explained by nonisolated polymer chains. Recall the compendium of turning times from dispersive to equilibrium triplet diffusion, plotted in Fig. 8. There seems to be no difference in t_s between the 10^{-4} diluted zeonex film and the 10^{-4} frozen solution on the one hand and the solid film on the other hand, although the chain number per unit volume between both systems should, in principle, differ by some four orders of magnitude. In accordance with intuitive reasoning, Ries *et al.*, employing Monte Carlo techniques, found that halving the site concentration results in an increase of t_s by about one order of magnitude in time.[19] Thus, translated to our situation, the difference should easily be visible even within experimental error. This is at variance to the unchanged turning times we observed experimentally, which further confirms the presence of polymer chain clusters or aggregates. Thus, all frozen solution experiments probe the bulk rather than isolated polymer chains. Finally, we note that one could also argue the other way round, such as was done by Hertel *et al.*,[9] starting from the assumption that the polymer chains are truly isolated in frozen solution. In this case the unchanged turning times when comparing frozen solution and film point to an intrachain nature of the triplet migration in both cases. This, however, is clearly disproved by the vanishingly small DF2 signal in liquid solution when looking in the same (first microsecond) time period.

V. CONCLUSIONS

In this work time-resolved delayed fluorescence and photoinduced triplet absorption of a conjugated polymer have been investigated in detail. The results are consistent

with predictions of theories relying on incoherent hopping in an energetic Gaussian-like distribution of localized states, exhibiting a variance of 41 meV. The triplet migration within this distribution evolves in two time regimes initially characterized by dispersive and subsequently by nondispersive diffusion. In the bulk in both time regimes, triplet-triplet annihilation is observed, which decays proportional to t^{-1} and t^{-2}, respectively, thereby reducing the initial triplet population by ≈50%. The surviving triplets are either immobilized in the DOS at low temperature or populate trap sites outside the DOS for higher temperature. In either case, they decay monomolecularly with a characteristic decay time of 1.4 s.

In the framework of this study, clear evidence is found supporting the interchain nature of the triplet migration. However, we could not gain an absolute (temperature-dependent) value for the triplet diffusivity. For this an emissive dopant is needed, which, unlike the currently used heavy metal containing phosphorescent dopants, traps the triplet excitons but does not capture singlet excitons by Forster transfer at the same time.

ACKNOWLEDGMENTS

We are deeply indebted to Professor U. Scherf for his ongoing and generous supply of polyfluorene. Professor H. D. Burrows contributed his chemical knowledge to this study. We are indebted to Professor Kadashchuk for his most useful preprint. The authors C.R. and A.P.M. acknowledge financial support from the Phillips Research Laboratories Eindhoven and by EPSRC (Grant No. GR/R 19687) and the Leverhyulme Foundation, respectively.

*Electronic address: carsten.rothe@dur.ac.uk

[1] M. Wohlgenannt *et al.*, Nature (London) **409**, 494 (2001).
[2] H. D. Burrows *et al.*, J. Chem. Phys. **115**, 9601 (2001).
[3] S. Sinha *et al.*, Phys. Rev. Lett. **90**, 127402 (2003).
[4] Y. V. Romanovskii *et al.*, Phys. Rev. Lett. **84**, 1027 (2000).
[5] C. Rothe and A. P. Monkman, Phys. Rev. B **65**, 073201 (2002).
[6] D. Hertel *et al.*, Adv. Mater. **13**, 65 (2001).
[7] A. Kadashchuk *et al.*, Chem. Phys. **291**, 243 (2003).
[8] C. Rothe *et al.*, J. Chem. Phys. **116**, 10503 (2002).
[9] D. Hertel *et al.*, J. Chem. Phys. **115**, 10007 (2001).
[10] C. Rothe *et al.*, J. Chem. Phys. **115**, 9557 (2001).
[11] D. Hertel *et al.*, Synth. Met. **116**, 139 (2001).
[12] T. Miteva *et al.*, Adv. Mater. **13**, 565 (2001).
[13] B. Lyons, S. I. Hintschich, and A. P. Monkman, J. Chem. Phys. (unpublished).
[14] A. J. Cadby *et al.*, Phys. Rev. B **62**, 15 604 (2000).
[15] R. Richert *et al.*, Philos. Mag. Lett. **59**, 95 (1989).
[16] B. Movaghar, B. Ries, and M. Grunewald, Phys. Rev. B **34**, 5574 (1986).
[17] B. Movaghar *et al.*, Phys. Rev. B **33**, 5545 (1986).
[18] M. Scheidler *et al.*, Chem. Phys. Lett. **225**, 431 (1994).
[19] B. Ries *et al.*, Phys. Rev. B **37**, 5508 (1988).
[20] B. Ries and H. Bassler, J. Mol. Electron. **3**, 15 (1987).
[21] M. Pope and C.E. Swenberg, *Electronic Processes in Organic Crystals and Polymers* (Oxford University, New York, 1999).
[22] M. von Smoluchowski, Z. Phys. Chem., Stoechiom. Verwandtschaftsl. **92**, 129 (1917).
[23] J. B. Birks, *Photophysics of Aromatic Molecules* (Wiley Interscience, London, 1970).
[24] M. Grunewald *et al.*, Philos. Mag. B **49**, 341 (1984).
[25] H. Cordes *et al.*, Phys. Rev. B **63**, 094201 (2001).
[26] G. Schonherr, H. Bassler, and M. Silver, Philos. Mag. B **44**, 369 (1981).
[27] A. I. Rudenko and H. Bassler, Chem. Phys. Lett. **182**, 581 (1991).
[28] L. Pautmeier, U. Rauscher, and H. Bassler, Chem. Phys. **146**, 291 (1990).
[29] A. P. Monkman *et al.*, Phys. Rev. Lett. **86**, 1358 (2001).
[30] P. M. Borsenberger, L. T. Pautmeier, and H. Bassler, Phys. Rev. B **46**, 12 145 (1992).
[31] J. Lange, B. Ries, and H. Bassler, Chem. Phys. **128**, 47 (1988).
[32] O. Epshtein *et al.*, Phys. Rev. Lett. **90**, 046804 (2003).
[33] A. P. Monkman *et al.*, Chem. Phys. Lett. **340**, 467 (2001).
[34] C. Silva *et al.*, J. Phys.: Condens. Matter **14**, 9803 (2002).
[35] R. Osterbacka, Phys. Rev. B **60**, R11 253 (1999).
[36] G. Fytas *et al.*, Macromolecules **35**, 481 (2002).